Direct Evaluation of Rare Events in Active Matter from Variational Path Sampling

Avishek Das, Benjamin Kuznets-Speck, and David T. Limmer

Direct evaluation of rare events in active matter from variational path sampling

Avishek Das,[1, *] Benjamin Kuznets-Speck,[2, *] and David T. Limmer[1, 3, 4, 5, †]

[1]*Department of Chemistry, University of California, Berkeley, CA, 94720, USA*
[2]*Biophysics Graduate Group, University of California, Berkeley, CA, 94720, USA*
[3]*Chemical Sciences Division, LBNL, Berkeley, CA, 94720, USA*
[4]*Material Sciences Division, LBNL, Berkeley, CA, 94720, USA*
[5]*Kavli Energy NanoSciences Institute, University of California, Berkeley, CA, 94720, USA*
(Dated: December 13, 2021)

Active matter represents a broad class of systems that evolve far from equilibrium due to the local injection of energy. Like their passive analogues, transformations between distinct metastable states in active matter proceed through rare fluctuations, however their detailed balance violating dynamics renders these events difficult to study. Here, we present a simulation method for evaluating the rate and mechanism of rare events in generic nonequilibrium systems and apply it to study the conformational changes of a passive solute in an active fluid. The method employs a variational optimization of a control force that renders the rare event a typical one, supplying an exact estimate of its rate as a ratio of path partition functions. Using this method we find that increasing activity in the active bath can enhance the rate of conformational switching of the passive solute in a manner consistent with recent bounds from stochastic thermodynamics.

The constituent agents of active matter– biomolecules, colloids, or cells– autonomously consume energy to fuel their motion.[1,2] Their resultant nonequilibrium states have non-Boltzmann phase-space densities and exhibit exotic structural and dynamical collective fluctuations, including motility-induced phase separation and swarming.[3–7] Within these nonequilbrium steady-states, fleeting fluctuations can free particles from external potentials,[8–10] nucleate stable phases from metastable ones,[11,12] and assemble passive objects.[13,14] The study of such rare dynamical events within active matter and the calculation of their associated rates is difficult. Traditional equilibrium rate theories like transition state theory and Kramer's theory require knowledge of the form of the steady-state distribution that is not in general available.[15] Further, only a few numerical methods exist that can be used to tame the exponential computational cost associated with sampling the unlikely fluctuations that lead to transitions between metastable states. Existing methods improve sampling by stratifying or branching stochastic trajectories[16–18] but do not typically employ driving forces to specifically enhance the sampling of these rare events.

Here we present a perspective and an associated numerical algorithm, termed Variational Path Sampling (VPS), for estimating transition rates in active systems using optimized time-dependent driving forces. Our approach relies on a equality between the rate of a rare event in a reference system and a ratio of path partition functions in the reference system and with a driving force that makes the rare event occur with high probability. The VPS algorithm solves a variational problem to approximate the functional form of an optimal time-dependent driving force for this estimate and is applicable to any stochastic dynamics. With VPS we investigate how driven fluids can direct motion into useful function.

We apply this technique to study the rate of conformational changes of a passive dimer in a dense bath of active Brownian particles.[19–21] This model exemplifies how collective active fluctuations around passive solutes can drive self-assembly and speed up transitions between distinct metastable states.[22,23] We find the rate to switch between the dimer's two metastable states increases dramatically with increasing activity in the bath, which we rationalize with a recent dissipation bound from stochastic thermodynamics.[24] We study the computational efficiency of rate estimation with VPS and demonstrate its advantage over existing trajectory stratification based methods like Forward Flux Sampling.[16]

We consider a system described by overdamped Brownian dynamics of the form,

$$\gamma_i \dot{\mathbf{r}}_i(t) = \mathbf{F}_i[\mathbf{r}^N(t)] + \boldsymbol{\eta}_i(t) \qquad (1)$$

where $\dot{\mathbf{r}}_i$ is the rate of change of the i-th particle's position, γ_i is the corresponding friction coefficient, and $\mathbf{F}_i[\mathbf{r}^N(t)]$ is the sum of all conservative, nonconservative and active forces exerted on the i-th particle that depends on the full configuration of the N-particle system, $\mathbf{r}^N$. The final term, $\boldsymbol{\eta}_i(t)$, is a Gaussian white-noise with $\langle \eta_{i\alpha}(t) \rangle = 0$ and

$$\langle \eta_{i\alpha}(t)\eta_{j\beta}(t') \rangle = 2\gamma_i k_{\mathrm{B}}T \delta_{ij}\delta_{\alpha\beta}\delta(t-t') \qquad (2)$$

for component (α, β) and $k_{\mathrm{B}}T$ is Boltzmann's constant times the temperature. In order to study the transition rate between two long-lived metastable states, denoted A and B, we define each from a given configuration using the indicator functions,

$$h_X[\mathbf{r}^N(t)] = \begin{cases} 1 & \text{if } \mathbf{r}^N(t) \in X \\ 0 & \text{else} \end{cases}, \qquad (3)$$

for either $X = A, B$. In practice this designation requires an order parameter capable of distinguishing configura-

tions and grouping them into these distinct metastable states like that illustrated in Fig. 1(a) in one dimension. Assuming there exists a separation between the time $\tau^{\ddagger}$ required to traverse the transition region between the two metastable states, and the typical waiting time for the transition, the rate k can be evaluated from the probability to observe a transition, per unit time[25]

$$k = \frac{\langle h_B(t_f) h_A(0) \rangle}{t_f \langle h_A \rangle} = t_f^{-1} \langle h_{B|A}(t_f) \rangle , \qquad (4)$$

where the angular brackets denote an average over trajectories of duration $\tau^{\ddagger} < t_f \ll 1/k$ started from a steady-state distribution in A and $\langle h_{B|A}(t_f) \rangle$ denotes the conditional probability for transitioning between A and B in time t_f. When t_f is chosen to satisfy the timescale separation described above, k is independent of time.

If the transition is rare, most short trajectories are nonreactive leading to difficulties in estimating the rate directly. Instead of trying to evaluate the small transition probability through stratification as other existing methods do,[16,17] we instead optimize a time-dependent driving force $\boldsymbol{\lambda}(\mathbf{r}^N, t)$ that constrains the transition to occur, and evaluate the probability cost associated with adding that force to the original dynamics. For a general time-dependent force $\boldsymbol{\lambda}$, using the Onsager-Machlup form for the probabilities of stochastic trajectories,[26] the rate expression in Eq. 4 can be rewritten as[24]

$$k = t_f^{-1} \left\langle e^{-\Delta U_{\boldsymbol{\lambda}}} \right\rangle_{B|A, \boldsymbol{\lambda}} , \qquad (5)$$

where $\langle \rangle_{B|A, \boldsymbol{\lambda}}$ denotes a conditioned average computed in presence of the additional force. This relation holds for forces $\boldsymbol{\lambda}$ that affect the transition to occur with probability 1, such that the rate in the driven ensemble is $1/t_f$. The average is of the exponential of the change in the path action, $\Delta U_{\boldsymbol{\lambda}}$,

$$\Delta U_{\boldsymbol{\lambda}}[\mathbf{X}] = -\int_0^{t_f} dt \sum_i \frac{[\boldsymbol{\lambda}_i^2 - 2\boldsymbol{\lambda}_i \cdot (\gamma_i \dot{\mathbf{r}}_i - \mathbf{F}_i)]}{4\gamma_i k_{\mathrm{B}} T} , \qquad (6)$$

between trajectories generated with the added force and in its absence. The path action and all other stochastic integrals are evaluated in the Ito convention.

Equation 5 is a direct estimator for a rate employing an auxiliary control system, but it only becomes useful when the protocol $\boldsymbol{\lambda}(\mathbf{r}^N, t)$ generates trajectories in a manner equivalent to the unbiased reactive trajectory distribution. This is because the expectation can be viewed as an overlap between the two reactive path distributions, and without significant overlap the exponential average is difficult to estimate. We express the optimality of $\boldsymbol{\lambda}$ using Jensen's inequality after taking the logarithm of Eq. 5 to obtain a variational principle,

$$\ln k \geq -\ln t_f - \langle \Delta U_{\boldsymbol{\lambda}} \rangle_{B|A, \boldsymbol{\lambda}} . \qquad (7)$$

If the average change in conditioned path action $\langle \Delta U_{\boldsymbol{\lambda}} \rangle_{B|A, \boldsymbol{\lambda}}$ is minimized over all possible functional
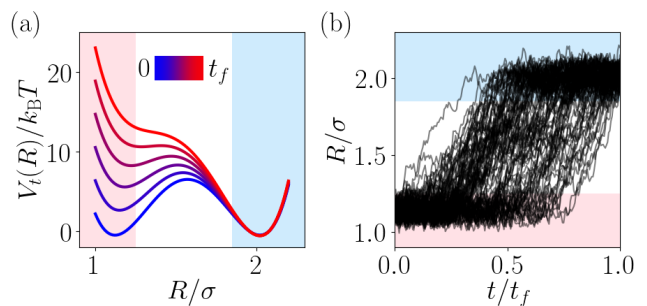
FIG. 1. Reactive trajectories with VPS. (a)Schematic representation of the total optimal time-dependent potential in an isolated passive dimer as t goes from 0 to t_f. Shaded regions are the compact (A, pink) and extended (B, light blue) states. (b) Unbiased reactive trajectories generated with $\boldsymbol{\lambda}(R, t)$.

forms of $\boldsymbol{\lambda}$, the rate can be obtained directly as a simple ensemble average of $\Delta U_{\boldsymbol{\lambda}^*}$ at the minimizer $\boldsymbol{\lambda} = \boldsymbol{\lambda}^*$.

The optimal control force $\boldsymbol{\lambda}^*$ that saturates Eq. 7 is unique and given by the solution of the backward Kolmogorov equation[27–29] as detailed in the Supporting Material(SM), which includes Refs. [6, 16, 24, 27–39]. Specifically, the optimal force is $2k_{\mathrm{B}}T$ times the gradient of the logarithm of the commitor probability[40] of ending in state B at t_f. A schematic illustration of the optimal effective time-dependent potential $V_t(R)$ added to a double well potential is illustrated in Fig. 1(a). The resultant force gradually destabilizes the reactant well to ensure the transition almost surely within the short duration t_f. Viewed in the backwards direction of time, the potential follows the negative logarithm of the relaxation of an initially localized distribution in B to its steady-state. The force is thus optimal in the sense that reactive trajectories, like those in Fig. 1(b), generated with it are drawn from the reference path ensemble with the correct statistical weights. Generically, $\boldsymbol{\lambda}^*(\mathbf{r}^N, t)$ is a function of all particle coordinates, so it is not typically tractable to compute. We demonstrate here that one- and two-body representations of $\boldsymbol{\lambda}$ can be sufficiently close to optimal as to estimate the rate accurately even in cases where the rare event is collective, similar to related observations in large-deviation sampling.[33,41–43]

We study the accuracy and utility of this formalism in a system comprised of an active bath and a passive dimer that can undergo conformational changes between two metastable states. All particles interact pairwise via a Weeks-Chandler-Andersen (WCA) repulsive potential[44]

$$V_{\mathrm{WCA}}(\mathbf{r}) = \left\{ 4\epsilon \left[\left(\frac{\sigma}{r}\right)^{12} - \left(\frac{\sigma}{r}\right)^6 \right] + \epsilon \right\} \Theta(r_{\mathrm{WCA}} - r) \qquad (8)$$

with energy scale ϵ, and particle diameter σ, truncated at $r_{\mathrm{WCA}} \equiv 2^{1/6}\sigma$ with the Heaviside function Θ. Active particles experience an additional self-propulsion force of magnitude v_0, $\mathbf{F}_i^a(t) = v_0 \mathbf{e}[\theta_i(t)]$ where the director is

$\mathbf{e}(\theta_i) = (\cos\theta_i, \sin\theta_i)$ and θ_i obeys $\dot{\theta}_i(t) = \xi_i(t)$ with,

$$\langle \xi_i(t) \rangle = 0, \quad \langle \xi_i(t)\xi_j(t') \rangle = 2D_\theta \delta_{ij}\delta(t-t') \qquad (9)$$

for angular diffusion constant D_θ. Passive solutes separated by distance R are bound by a double-well potential

$$V_{\mathrm{dw}}(R) = \Delta V \left[1 - (R - r_{\mathrm{WCA}} - w)^2/w^2 \right]^2 \qquad (10)$$

with an energy barrier of height ΔV between the compact and extended states at $R = r_{\mathrm{WCA}}$ and $R = r_{\mathrm{WCA}} + 2w$ respectively.[45] We study the transition rates between these states, employing indicator functions $h_A(t) = \Theta(R_A - R)$ and $h_B(t) = \Theta(R - R_B)$ for $R_A = 1.25\sigma$ and $R_B = 1.85\sigma$. Conformation transitions like these in dense fluids are collective in origin[45] and serve as a sensitive probe of the bath.

The VPS algorithm estimates an optimal force using a low-rank ansatz by iteratively solving the variational problem in Eq. 7, and uses this force to directly obtain a rate estimate. For computing the rate of isomerization of the passive dimer, we approximate $\boldsymbol{\lambda}^*$ with a time-dependent interaction along the dimer bond vector $\mathbf{R}$, expressed as a sum of Gaussians

$$\boldsymbol{\lambda}(\mathbf{R},t) = \hat{\mathbf{R}} \sum_{p,q=1}^{M_R, M_t} c_{pq}^{(i)} e^{-\frac{(R-\mu_{R,p})^2}{2\nu_R^2} - \frac{(t-\mu_{t,q})^2}{2\nu_t^2}} \qquad (11)$$

where $c_{pq}^{(1)} = -c_{pq}^{(2)}$ are variational parameters to be tuned, and the locations and widths $\mu_{R,p}$, $\mu_{t,q}$, ν_R and ν_t are held fixed. To impose the conditioning while minimizing $\langle \Delta U_{\boldsymbol{\lambda}} \rangle_{B|A,\boldsymbol{\lambda}}$, we use a Lagrange multiplier s to construct a loss function $\Omega_{\boldsymbol{\lambda}} = \langle \Delta U_{\boldsymbol{\lambda}} \rangle_{\boldsymbol{\lambda}} + s(\langle h_{B|A} \rangle_{\boldsymbol{\lambda}} - 1)$. For a general force that does not ensure the transition with unit probability, there is a multiplicative contribution to the estimate of the rate in Eq. 5 from $\langle h_{B|A} \rangle_{\boldsymbol{\lambda}}$, which for most optimized forces is negligible.

The optimization problem maps onto the computation of a cumulant generating function for the statistics of the indicator $h_B(t_f)$ studied previously,[29,32] with the short trajectories starting from a steady-state distribution in the initial state. As such we can employ generalizations of recent reinforcement learning procedures to efficiently estimate the gradients of the loss function with respect to the variational parameters.[46] Specifically, we modify the Monte-Carlo Value Baseline (MCVB) algorithm[32] which performs a stochastic gradient descent to optimize $c_{pq}^{(i)}$. We add two preconditioning steps over the MCVB algorithm. First, we generate an initial reactive trajectory using a routine reminiscent of well-tempered metadynamics.[35] Then we symmetrize the learned force to ensure time translational invariance of the transition paths. We denote this preconditioning algorithm MCVB-T. Further information is available in the SM.

We first illustrate the systematic convergence of VPS by estimating the isomerization rate of an isolated passive
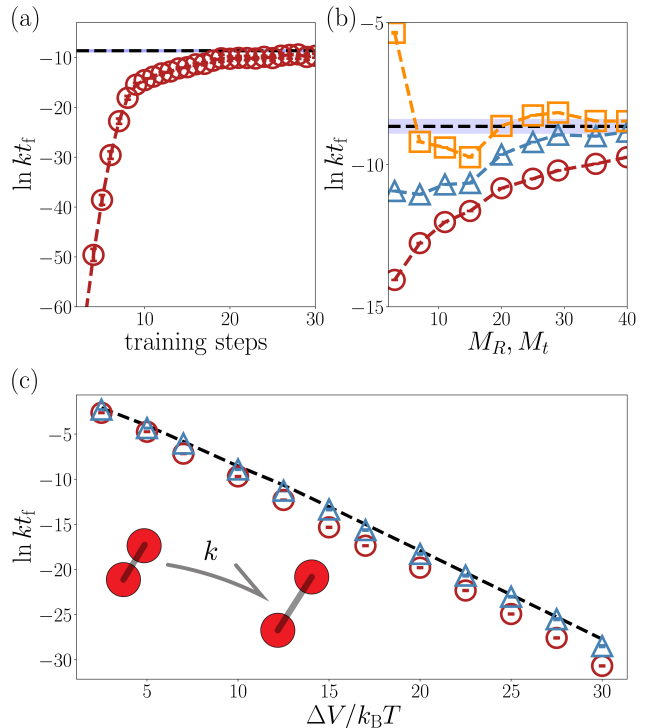
FIG. 2. Convergence of isomerization rates for an isolated passive dimer. (a) Learning curve for $\Delta V = 10k_{\mathrm{B}}T$ and $M_R, M_t = 20$. (b) Convergence of the variational rate estimate (circles) and cumulant corrections for $\ell = 2$ (triangles) and $\ell = 4$ (squares) with basis size as compared to the numerically exact answer (dashed line). (c) Variational (circles) and $\ell = 2$ (triangles) estimate of the rate compared to the exact value (dashed line) with increasing barrier height.

dimer. Such a simplified system allows us to compare to numerically exact results, and study convergence of the force ansatz in the complete basis limit, where $M_R, M_t \to \infty$ and the Gaussians cover the thermally sampled region in R and t. For this simple system, we take $k_{\mathrm{B}}T = \gamma = \sigma = \epsilon = 1$, $w = 0.25\sigma$, with diffusive timescale $\tau = \sigma^2\gamma/k_{\mathrm{B}}T$. We simulate the one-dimensional version of Eq. 1 along R, with $V_{\mathrm{dw}}(R)$ only. For simplicity we define state A by the initial condition $R(0) = r_{\mathrm{WCA}}$, and state B via $R_B = 1.45\sigma$. To provide a steady-state value in Eq. 4,[32,47] we use an Euler method and take in this example $t_f = \gamma w\sigma/\sqrt{8k_{\mathrm{B}}T\Delta V}$. We choose $\mu_{R,p}$ and $\mu_{t,q}$ evenly distributed in $R/\sigma \in [0.9, 1.77]$ and $t \in [0, t_f]$, respectively, and ν_R, ν_t to be half the distance between Gaussian centers. We consider basis sizes $M_R = M_t = 2 - 40$, each optimized independently and used to sample $\sim 10^5$ transition paths.

Figure 2(a) illustrates a typical learning curve for the control force, showing convergence of the variational rate bound towards the numerically exact rate. The variational estimate requires a basis of $M_R, M_t > 40$ to approach the rate to within the statistical uncertainty of

the estimate, however alternative estimates with small basis sets can be refined using a cumulant expansion approximation to Eq. 5. Specifically, truncating the exact exponential relation at the ℓth cumulant as

$$\ln k \approx -\ln t_f + \sum_{n=1}^{\ell} \frac{1}{n!} \frac{d^n \ln \langle e^{-\Delta U_{\boldsymbol{\lambda}}} \rangle_{B|A,\boldsymbol{\lambda}}}{d\Delta U_{\boldsymbol{\lambda}}^n} \qquad (12)$$

provides an approximation to the rate that converges in the limit that ℓ is large. Figure 2(b) illustrates this convergence, where we find that even coarse-representations of the control force can yield close estimates of the rate with only the first few cumulants, illustrating a tradeoff between basis set completeness and statistical efficiency. Sweeping across a wide range of barrier heights in Fig. 2(c), we find excellent agreement between the log-rate from brute force simulations and a truncation of the cumulant expansion to $\ell = 2$ using $M_R = 80$ and $M_t = 30$.

We next compute the isomerization rate with VPS when the dimer is immersed in an explicit solvent of active Brownian particles with $N = 80$ and a total density of $0.6/\sigma^2$. The dimer particles have a friction $\gamma_{\mathrm{d}} = 2\gamma$ and the solvent particles have $\gamma_{\mathrm{s}} = 4\gamma$. We take $\gamma = \sigma = \epsilon = 1$, $k_{\mathrm{B}}T = 0.5$, $\Delta V = 7k_{\mathrm{B}}T$, $\tau = \sigma^2\gamma/2k_{\mathrm{B}}T = 1$, $D_\theta = 1/\tau$ and timestep $10^{-5}\tau$. We also change $w = 0.45\sigma$ such that the collisional cross-section of the dimer is large. Collisions with active particles transduce energy along the dimer bond and we study the change in the isomerization rate as the bath activity $v_0\sigma/k_{\mathrm{B}}T$ is varied from 0 to 18. We use a basis size of $M_R = M_t = 50$ distributed between $R/\sigma \in [0.9, 2.3]$ and $t \in [0, t_f]$ where $t_f = 0.2\tau$. The optimization starts by learning forces $\boldsymbol{\lambda}(\mathbf{R}, t)$ for the isolated dimer with WCA interactions between monomers, followed by the MCVB-T algorithm. Then, $\boldsymbol{\lambda}(\mathbf{R}, t)$ is optimized in the presence of the bath for $v_0 = 0$ and higher values of v_0 are initialized from converged forces at the previous v_0.

The rate is a strong function of activity, increasing twenty-fold over the range of v_0's considered. While the variational rate estimate from Eq. 7 is closest for the passive bath, it weakens with increasing v_0, indicating a growing importance of solvent degrees of freedom in the optimal control force. With converged forces at each v_0, we run 10^6 trajectories of length t_f to compute k from Eq. 5. This estimate correctly predicts the suppression of k due to passive solvation and can be converged statistically for $v_0\sigma/k_{\mathrm{B}}T < 9$, which is supported by direct rate estimates from unbiased simulations in Fig. 3(a). Above $v_0\sigma/k_{\mathrm{B}}T = 9$, the optimized force is not close enough to $\boldsymbol{\lambda}^*$ to estimate k directly through the exponential average or a low order cumulant expansion.

Provided we have access to the transition path ensemble from direct unbiased simulations or methods like Transition Path Sampling[48–50] we can supplement the estimate of k using histogram reweighting.[51] k satisfies a
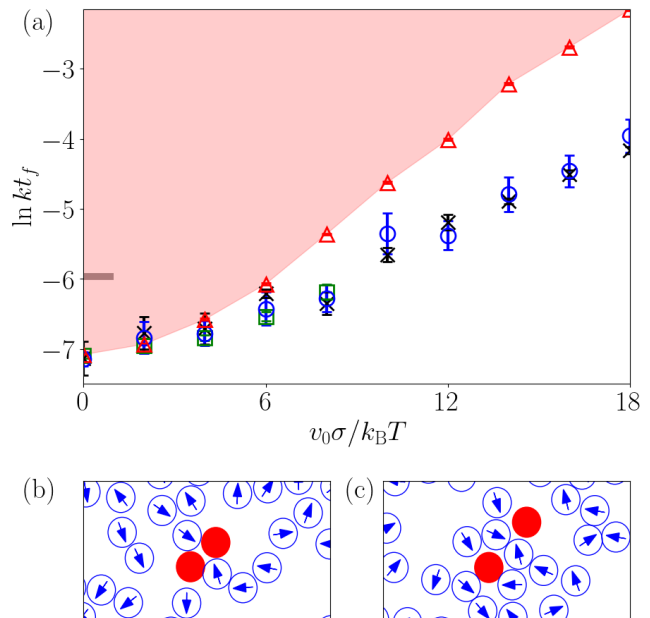
FIG. 3. Rate enhancement of isomerization in an active fluid. (a) Change in the rate as estimated from direct unbiased simulations (crosses), from exponential estimate (squares), and from histogram reweighting (circles). The excess dissipated heat (triangles) bounds the rate enhancement achievable demarked by the red shaded region. The thick tick mark on the left denotes the rate for the isolated dimer. (b) and (c) Typical snapshots of reactive trajectories of the active bath (blue) and passive dimer (red), at $t = 0$ and $t = t_f$.

reweighting relation of the form,

$$k = \frac{e^{-\Delta U_{\boldsymbol{\lambda}}} P_{B|A,\boldsymbol{\lambda}}(\Delta U_{\boldsymbol{\lambda}})}{t_f P_{B|A,0}(\Delta U_{\boldsymbol{\lambda}})} \qquad (13)$$

where we have defined $P_{B|A,\boldsymbol{\lambda}}(\Delta U_{\boldsymbol{\lambda}}) = \langle \delta(\Delta U_{\boldsymbol{\lambda}}[\mathbf{X}] - \Delta U_{\boldsymbol{\lambda}}) \rangle_{B|A,\boldsymbol{\lambda}}$ and similarly for its undriven counterpart $\boldsymbol{\lambda} = 0$. We evaluate k with this estimator by sampling 10^4 driven and only 6-100 unbiased reactive paths, using the Bennett Acceptance Ratio[36] to evaluate the ratio of probabilities. Compared with the brute-force estimate in Fig. 3(a), we find this reweighting predicts k accurately across all values of v_0 with significantly higher statistical efficiency then a brute force calculation, which validates the accuracy and utility of the control forces. We have compared the VPS rate estimates in the SM, using either Eqs. 5 and 13, to the Rosenbluth variant of Forward Flux Sampling,[16] and find that VPS is statistically more efficient and converges more quickly with the number of reactive trajectories.

Access to an ensemble of transition paths in this active system gains us mechanistic insight into the process. The rate enhancement observed for the compact to extended state transition of the passive dimer with bath activity can be understood using recent results from stochastic thermodynamics. Specifically the rate enhancement

achievable by coupling a reactive mode to a nonequilibrium driving force is bounded from above by the heat dissipated over the course of the transition.[24] In this case the nonequilibrium driving is afforded by the interactions between the dimer and the active bath, so the bound takes the form

$$\ln k \leq \ln k_0 + \frac{1}{2k_{\mathrm{B}}T}\langle Q - Q_0 \rangle_{B|A} \qquad (14)$$

where k_0 is the rate at $v_0 = 0$ and $\langle Q - Q_0 \rangle_{B|A}$ is the dissipative heat less its average at $v_0 = 0$ given by

$$Q = \int_0^{t_f} dt \sum_{i \in \mathrm{d}} \sum_{j \in \mathrm{s}} (\dot{\mathbf{r}}_i - \dot{\mathbf{r}}_j) \cdot \mathbf{F}_{\mathrm{WCA}}(\mathbf{r}_{ij}) \qquad (15)$$

which is a sum of the total force from the WCA potential of the solvent particles (s) on the dimer (d) times the difference in their velocities in an ensemble at fixed v_0 (SM). This bound is verified in Fig. 3(a) for all v_0, and saturated at small v_0. The specific mechanism of energy transfer from bath to dimer that promotes transitions is clarified by examining reactive trajectories driven by the biasing force and are typical, after removal of the bias from the incomplete basis set. Figures 3 (b) and (c) show typical snapshots of the solvated dimer at the start and end of the reaction. Energy transfer results from active particles accumulating around the dimer, and preferentially in its cross-section, pushing it apart into an extended state. This mechanism of action is reminiscent of how nonequilibrium agents collect in the corners of mesoscopic gears to power their directed rotation.[22,23] At low v_0, we find the driven isomerization process is efficient, while deviation from the bound at large v_0 demonstrates that energy is additionally funneled into non-reactive modes. Further studies showing the unbiased nature of the VPS-sampled transition path ensemble in terms of duration and distribution of transition paths, and quantification of the changing solvation environment with v_0 are provided in the SM.

In conclusion, we developed a novel formalism and corresponding algorithm termed Variational Path Sampling to compute rate constants in nonequilibrium systems by optimally driving the systems to transition between metastable states. VPS can be used to compute rates in arbitrary stochastic systems and extends the use of optimal control forces in large deviation sampling to transient rare events.[29,33,41,42,52] VPS complements trajectory-level importance sampling methods by generating the rare reactive event through a time-series of driving forces instead of a sequence of rare noise histories. We expect this approach to find broad use in rate computations for rare events in dissipative systems throughout the physical sciences and across scales.

* These authors contributed equally
† dlimmer@berkeley.edu

[1] M. C. Marchetti, J.-F. Joanny, S. Ramaswamy, T. B. Liverpool, J. Prost, M. Rao, and R. A. Simha, Reviews of Modern Physics **85**, 1143 (2013).

[2] M. R. Shaebani, A. Wysocki, R. G. Winkler, G. Gompper, and H. Rieger, Nature Reviews Physics **2**, 181 (2020).

[3] M. E. Cates and J. Tailleur, Annual Reviews of Condensed Matter Physics **6**, 219 (2015).

[4] T. Speck, The European Physical Journal Special Topics **225**, 2287 (2016).

[5] T. Nemoto, É. Fodor, M. E. Cates, R. L. Jack, and J. Tailleur, Physical Review E **99**, 022605 (2019).

[6] T. GrandPre, K. Klymko, K. K. Mandadapu, and D. T. Limmer, Physical Review E **103**, 012613 (2021).

[7] G. Gompper, R. G. Winkler, T. Speck, A. Solon, C. Nardini, F. Peruani, H. Löwen, R. Golestanian, U. B. Kaupp, L. Alvarez, *et al.*, Journal of Physics: Condensed Matter **32**, 193001 (2020).

[8] E. Woillez, Y. Zhao, Y. Kafri, V. Lecomte, and J. Tailleur, Physical review letters **122**, 258001 (2019).

[9] A. Militaru, M. Innerbichler, M. Frimmer, F. Tebbenjohanns, L. Novotny, and C. Dellago, Nature Communications **12**, 1 (2021).

[10] E. Woillez, Y. Kafri, and V. Lecomte, Journal of Statistical Mechanics: Theory and Experiment **2020**, 063204 (2020).

[11] A. K. Omar, K. Klymko, T. GrandPre, and P. L. Geissler, Physical Review Letters **126**, 188002 (2021).

[12] D. Richard, H. Löwen, and T. Speck, Soft Matter **12**, 5257 (2016).

[13] J. Stenhammar, R. Wittkowski, D. Marenduzzo, and M. E. Cates, Physical review letters **114**, 018301 (2015).

[14] S. A. Mallory, C. Valeriani, and A. Cacciuto, Annual review of physical chemistry **69**, 59 (2018).

[15] A. Nitzan, *Chemical dynamics in condensed phases: relaxation, transfer and reactions in condensed molecular systems* (Oxford university press, 2006).

[16] R. J. Allen, C. Valeriani, and P. R. Ten Wolde, Journal of physics: Condensed matter **21**, 463102 (2009).

[17] A. Warmflash, P. Bhimalapuram, and A. R. Dinner, The Journal of chemical physics **127**, 114109 (2007).

[18] F. Cérou and A. Guyader, Stochastic Analysis and Applications **25**, 417 (2007).

[19] Y. Fily and M. C. Marchetti, Physical review letters **108**, 235702 (2012).

[20] G. S. Redner, M. F. Hagan, and A. Baskaran, Physical review letters **110**, 055701 (2013).

[21] J. Bialké, H. Löwen, and T. Speck, Europhysics Letters **103**, 30008 (2013).

[22] S. Mallory, M. Bowers, and A. Cacciuto, The Journal of Chemical Physics **153**, 084901 (2020).

[23] A. Sokolov, M. M. Apodaca, B. A. Grzybowski, and I. S. Aranson, Proceedings of the National Academy of Sciences **107**, 969 (2010).

[24] B. Kuznets-Speck and D. T. Limmer, Proceedings of the National Academy of Sciences **118** (2021).

[25] D. Chandler, The Journal of Chemical Physics **68**, 2959 (1978).

[26] L. Onsager and S. Machlup, Phys. Rev. **91**, 1505 (1953).

[27] J. Szavits-Nossan and M. R. Evans, Journal of Statistical Mechanics **2015**, P12008 (2015).

[28] R. Chetrite and H. Touchette, Annales Henri Poincar **16**, 2005 (2015).

[29] R. Chetrite and H. Touchette, Journal of Statistical Mechanics **2015**, P12001 (2015).

[30] S. N. Majumdar and H. Orland, Journal of Statistical Mechanics: Theory and Experiment **2015**, P06039 (2015).

[31] F. Carollo, J. P. Garrahan, I. Lesanovsky, and C. Pérez-Espigares, Physical Review A **98**, 010103 (2018).

[32] A. Das, D. C. Rose, J. P. Garrahan, and D. T. Limmer, arXiv:2105.04321 (2021).

[33] A. Das and D. T. Limmer, Journal of Chemical Physics **151**, 244123 (2019).

[34] P. Warren and R. Allen, Entropy **16**, 221 (2013).

[35] A. Barducci, G. Bussi, and M. Parrinello, Physical Review Letters **100**, 020603 (2008).

[36] M. R. Shirts and J. D. Chodera, Journal of chemical physics **129**, 124105 (2008).

[37] R. Zwanzig, *Nonequilibrium statistical mechanics* (Oxford university press, 2001).

[38] R. J. Allen, P. B. Warren, and P. R. Ten Wolde, Physical review letters **94**, 018104 (2005).

[39] R. J. Allen, D. Frenkel, and P. R. ten Wolde, The Journal of chemical physics **124**, 024102 (2006).

[40] E. Vanden-Eijnden *et al.*, Annual review of physical chemistry **61**, 391 (2010).

[41] U. Ray, G. K.-L. Chan, and D. T. Limmer, Physical review letters **120**, 210602 (2018).

[42] T. Nemoto, F. Bouchet, R. L. Jack, and V. Lecomte, Physical Review E **93**, 062123 (2016).

[43] D. Jacobson and S. Whitelam, Physical Review E **100**, 052139 (2019).

[44] J. D. Weeks, D. Chandler, and H. C. Andersen, The Journal of chemical physics **54**, 5237 (1971).

[45] C. Dellago, P. G. Bolhuis, and D. Chandler, The Journal of chemical physics **110**, 6617 (1999).

[46] D. C. Rose, J. F. Mair, and J. P. Garrahan, New Journal of Physics **23**, 013013 (2021).

[47] M. Delarue, P. Koehl, and H. Orland, The Journal of chemical physics **147**, 152703 (2017).

[48] P. G. Bolhuis, D. Chandler, C. Dellago, and P. L. Geissler, Annual review of physical chemistry **53**, 291 (2002).

[49] U. Ray, G. K.-L. Chan, and D. T. Limmer, Journal of chemical physics **148**, 124120 (2018).

[50] P. Buijsman and P. Bolhuis, The Journal of chemical physics **152**, 044108 (2020).

[51] D. Frenkel and B. Smit, *Understanding molecular simulation: from algorithms to applications*, Vol. 1 (Elsevier, 2001).

[52] J. Dolezal and R. L. Jack, Journal of Statistical Mechanics: Theory and Experiment **2019**, 123208 (2019).

[53] A. Das, B. Kuznets-Speck, and D. T. Limmer, "Direct evaluation of rare events in active matter from variational path sampling," (2021).